SULFUR IN THE EARLY MARTIAN ATMOSPHERE REVISITED: EXPERIMENTS WITH A 3-D GLOBAL CLIMATE MODEL.

L. Kerber, F. Forget, *Laboratoire de Météorologie Dynamique du CNRS, Université Paris 6, Paris, France (Kerber@lmd.jussieu.fr)*, **R. Wordsworth,** *Department of Geosciences, University of Chicago, Chicago, Illinois 60637, USA.*

Introduction:

Data returned from the surface of Mars during the 1970s revealed intriguing geological evidence for a warmer and wetter early martian climate. Dendritic valley networks were discovered by Mariner 9 on ancient Noachian terrain [1], indicating that liquid water had flowed across the surface in the distant past. Since this time, geological investigations into early Martian history have attempted to ascertain the nature and level of activity of the early Martian hydrological cycle [e.g. 2-5] while atmospheric modeling efforts have focused on how the atmosphere could be warmed to temperatures great enough to sustain such activity [see 6-7 for reviews].

Geological and spectroscopic investigations have refined the history and chronology of Noachian Mars over time, and circulation of liquid water has been invoked to explain several spatially and temporally distinct morphological and chemical signatures found in the geological record. Detections of iron and magnesium-rich clays are widespread in the oldest Martian terrains, suggesting a period of pH-neutral aqueous alteration [e.g., 8]. Valley network incision also took place during the Noachian period [9]. Some chains of river valleys and craters lakes extend for thousands of kilometers, suggesting temperatures at least clement enough for sustained ice-covered flow [3, 10]. The commencement of valley network incision is not well constrained, but the period of Mg/Fe clay formation appears to have ended before the termination of valley network formation, as the visible fluvial systems appear to have remobilized existing clays rather than forming them [5,8]. There is also evidence that the cessation of valley network formation was abrupt [11]. Towards the end of the Noachian, erosion rates appear to have been significantly higher than during subsequent periods, a process that has also been attributed to aqueous processes [12]. A period of sulfate formation followed, likely characterized by acidic, evaporitic playa environments [8].

A successful working model for the early Martian atmosphere and hydrosphere must be able not only to produce conditions suitable for liquid water at the surface, but also to explain how the nature of this aqueous activity changed over time and eventually diminished. There are two major end-member hypotheses: first, that early Mars was wet and warm, with a sustained greenhouse that made it possible for liquid water to be stable on the surface for extended periods [e.g., 2, 12-14], and second, that early Mars was generally cold, and that most of the aqueous alteration took place underground [3,5] or during transient warm periods tied to impact cratering [15], or volcanism [16]. In both the warm and cold scenarios, it is generally agreed that in order to make valley networks and sulfate deposits, a hydrological cycle is needed which is able to recycle water from the lowlands back to the highlands (i.e., the one-time emptying of a regional aquifer would not be sufficient to create the observed features) [4,17]. In both cases, volcanic gases (especially SO_2) have been suggested as a possible way of creating either a sustained or transient greenhouse. Several researchers have tested the addition of SO_2 to climate models in order to assess whether it would provide an adequate amount of greenhouse warming to allow liquid water to flow across the surface [18-21], with differing results. Postawko and Kuhn [18] found a warming effect of 14 K in a 0.1 bar atmosphere with an SO_2 abundance of 1000 ppm. A total greenhouse warming effect of 44 K was found using the same mixing ratio in a much thicker atmosphere (1 bar). Johnson et al. [20] and later Mischna et al. [19] used a 3-D global circulation model and found a warming of 15-25 K for 245 ppm of SO_2 in a dry 0.5 bar atmosphere [20] and 28 K for a saturated 0.5 bar atmosphere [19]. Tian et al. [21] used a 1-D model to explore a wide range of SO_2 mixing values and CO_2 partial pressures, finding a warming of around ~25 K for 100 ppm in a 0.5 bar atmosphere with a fully saturated troposphere (~40 K for a 1 bar atmosphere). These authors also included the effect of sulfate aerosol particles, which caused a dramatic cooling effect which more than canceled the warming caused by the SO_2 gas [21].

Here we reconsider the efficacy of a sulfur-induced greenhouse in early Noachian history using the LMD (Laboratoire de Météorologie Dynamique) 3-D Generic Climate Model (LMD-GCM), exploring the effects of SO_2, H_2S gases and sulfate and sulfur aerosols on the surface temperature. We intend to test and expand upon earlier works, using improved CO_2 spectroscopy, radiatively active CO_2 ice clouds, and more complete S_8 optical properties. The goals for this work are to determine:

(1) Whether (and by how much) SO_2 and H_2S were capable of warming the early Martian surface.

(2) How SO_2-derived warming varies depending on location on the planet, and how that compares to the spatial distribution of valley networks and aqueous mineral deposits.

(3) Whether (and by how much) sulfate and el-

emental sulfur aerosols were capable of cooling the Martian surface.

Methods: The GCM used in this study was developed for general planetary applications, and includes generalized radiative transfer and cloud physics [e.g., 22]. The model was adapted specifically to early Mars conditions and used by Forget et al. [7] to explore the effects of a CO_2 atmosphere from 0.1 to 7 bars, including the effects of different obliquities, orbital parameters, cloud microphysical parameters, atmospheric dust loading, and surface properties. This paper and a companion paper exploring the effects of a full water cycle including surface-atmosphere interactions and water ice clouds [23] concluded that even with the greenhouse warming provided by water vapor and water-ice clouds, above-freezing conditions were not met for sustained periods. Importantly, these results suggest that even if a thick CO_2-only atmosphere could be prevented from being drawn down into carbonate deposits [14], it would still not provide sufficient warming for sustained above-freezing temperatures.

Simulations were run at 0.5 bars with a 32x32x15 grid, corresponding to a resolution of 11.25º longitude by 5.625º latitude in the horizontal with 15 vertical levels from the surface to ~50 km. Other resolutions and pressures were also explored, and will be presented elsewhere. The correlated-k method was used to produce a database of coefficients for use by the radiative transfer code, using 80 spectral bands in the longwave and 36 in the shortwave. Real and imaginary indices for H_2SO_4 were taken from the HITRAN database, using the values from [24] for wavelengths between 0.2 and 0.337 μm and between 25 μm and 50 μm, while results from [25] were used for wavelengths between 0.360 μm and 25 μm (following [21] to allow for comparison). Improved S_8 optical indices (from the X-ray range out to 50 μm) were taken from Fuller et al. [1998]. Simulations with H_2O were run with a relative humidity profile derived from the full, self-consistent water cycle (including CO_2 and water ice clouds) used in [23]. The relative humidity in this profile is 45% near the surface with the hygropause near 8 km.

Results:

The Average Effect of Sulfur-Bearing Gases

Simulations were run in both dry and wet CO_2 atmospheres with various SO_2 and H_2S mixing ratios: 0 ppmv, 10 ppmv, 100 ppmv, 1000 ppmv, and 10000 ppmv (**Figure 1**). Where H_2O was included, the parameterized relative humidity profile described above was used. Two other relative humidity profiles were also tested: a fully saturated profile and an Earth-like relative humidity [27,28]. The saturated profile led to global annual average temperatures about 1-3 K higher than the parameterized profile, while the Earth-like profile led to temperatures 1-2 K lower. The addition of water vapor increases the greenhouse effect of the SO_2, but global average annual temperatures are still below freezing. For simulations with both H_2S and SO_2, the given amount of gas was added for each individual gas (e.g., 100 ppmv of gas corresponds to 100 ppmv of H_2S and 100 ppmv of SO_2).

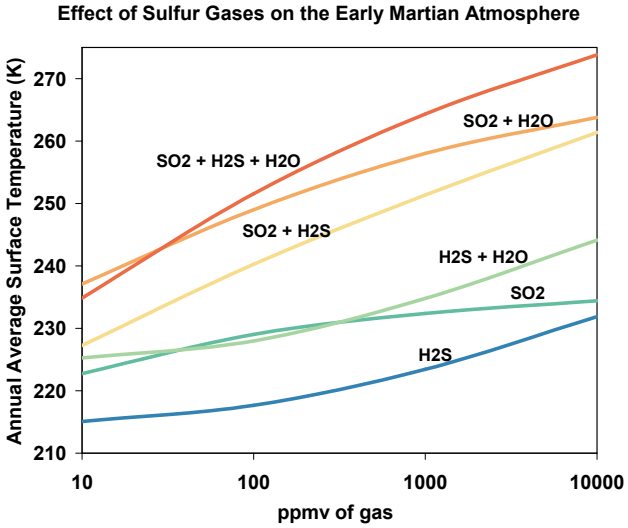

Figure 1.

Even in the cases where large amounts of SO_2 and H_2S are added to the atmosphere, the annual global average surface temperature does not rise above freezing. H_2S provides significantly less warming than SO_2.

Spatial Variability of SO_2 Warming

While average temperatures might not allow melting, regional and seasonal temperatures can be much higher. **Figure 2** shows maps of average annual surface temperature for different scenarios: CO_2 only, H_2O+CO_2, CO_2+SO_2 (100 ppmv), and CO_2+H_2O+SO_2 (100 ppmv). The parameterized water profile described above was used for the cases with water vapor. Significant warming is observed in Hellas Basin and around 30ºN, though the warmest areas do not coincide with the locations of the valley networks.

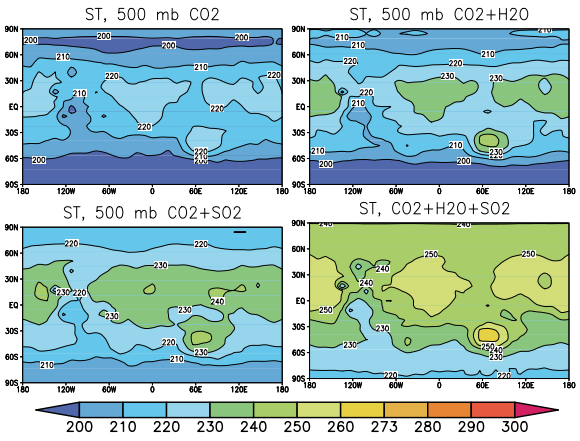

Figure 2.

While the average annual temperature provides a general idea about the spatial variability of possible melting, it is likely that temperatures will fluctuate depending on the time of year or day. **Figures 3a** and **3b** show the fraction of the year that temperatures rise above freezing on the surface (without and with 100 ppmv of SO_2, respectively). Without SO_2, the temperature of the surface rises above freezing for about 10% of the year at the bottom of Hellas Basin. With 100 ppmv of SO_2, Hellas spends 40% of its time above freezing, and places in the northern plains spend up to 30% of their time above freezing. **Figure 3c** shows the fraction of the year for which the daily average temperature is above zero. This is a useful metric because a warm season during which water stays liquid for many hours would likely lead to more efficient erosion than a season during which melting was reached for only an hour each day, for example. Once again, the greatest warming takes place at the bottom of Hellas Basin and in the deepest parts of the Northern Plains.

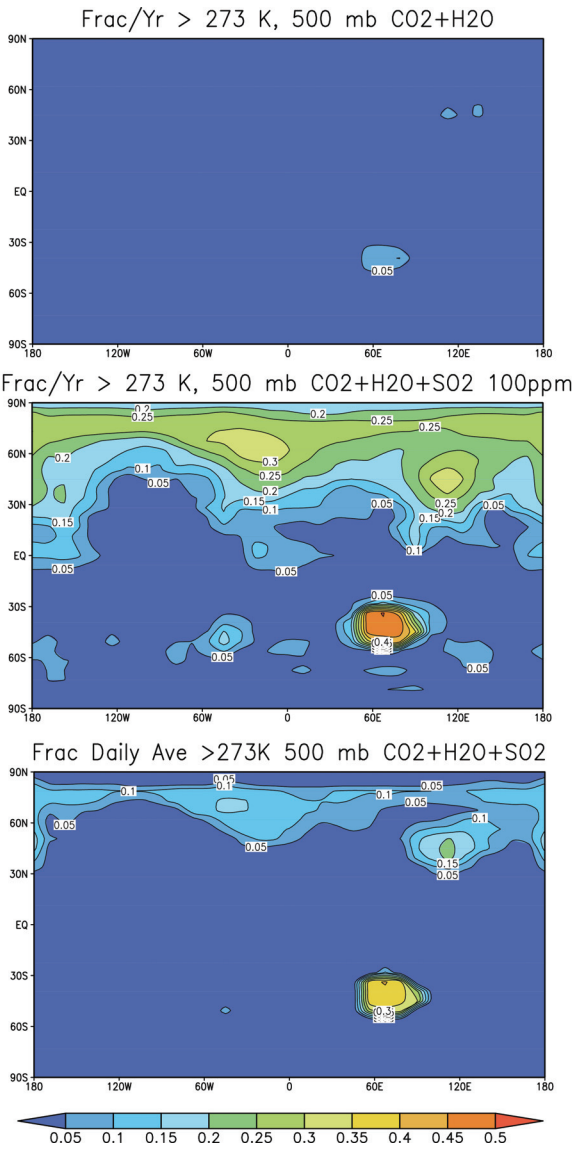

Figure 3.

In this "best case scenario", where warming sulfur-bearing gases accumulate in the atmosphere and no cooling aerosols form, some parts of the planet can sustain above-freezing temperatures for considerable fractions of the year. However, the parts of the planet where valley networks and aqueous minerals are found coincide with some of the coldest parts of the planet, where temperatures rarely rise above freezing, even on the warmest days.

The Effect of Sulfur and Sulfate Aerosols

In order to determine the likely effect of sulfate and elemental sulfur aerosol formation, it is necessary to see how much the surface is cooled given a particular aerosol optical depth, and also to determine how much aerosol is required to create each optical depth. Aerosol simulations were first run in a dry CO_2 atmosphere with well-mixed 1 μm H_2SO_4 or S_8 particles with opacities ranging from τ= 0.2 to 10 (at 550 nm). These produced cooling from a few degrees to ~23 K for H_2SO_4 τ= 10 (**Figure 4**). A single layer of H_2SO_4 aerosols of the same opacity produced similar results.

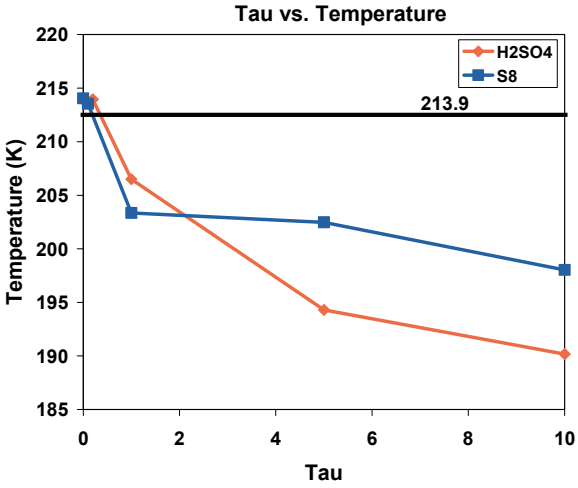

Figure 4.

Holding the opacity constant and varying the particle size reveals that small particles cool strongly, while larger particles produce less cooling and very large particles (10 μm) producing significant warming (**Figure 5**). On Earth, H_2SO_4 aerosols tend to be between 0.1 μm and 1 μm in the accumulation mode [e.g., 29], so the net effect of these aerosols would most likely be cooling. It is theoretically possible for S_8 aerosols to grow to larger sizes, as small liquid droplets in equilibrium with their own vapor will tend to evaporate and recondense on larger particles [30]. However, Tian et al. [21], using a model comparing the relative timescales for nucleation, coagulation, and sedimentation, estimated a particle size around 0.2 μm for S_8 aerosols.

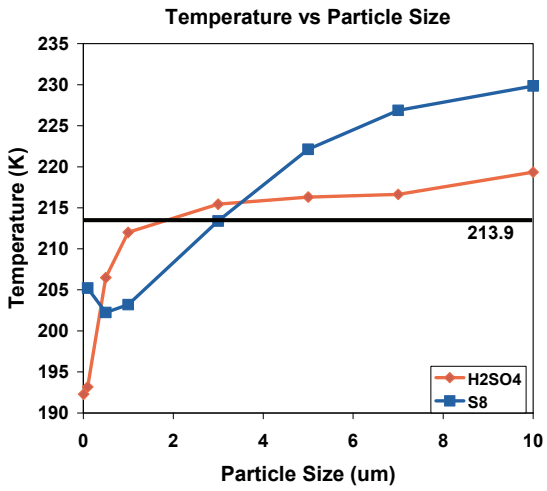

Figure 5.

Most importantly, while a significant amount of SO_2 gas is required to create a moderate amount of surface warming, only a very small amount of aerosol is needed for dramatic cooling. For example, if 100 ppmv of SO_2 was released into the atmosphere, and only 0.04% of it became 0.1-μm $_{H2SO4}$ particles, the entire warming effect of the SO_2 would be cancelled out. **Figure 6** shows the cooling effects of sulfate and sulfur aerosols versus the mixing ratio in ppmv of equivalent H_2SO_4 or S_8 gas. Each line ends at the mixing ratio which creates an optical depth of 10 (at 550 nm). The green line shows the combined effect of 100 ppmv of SO_2 with rising amounts of H_2SO_4 aerosol. The warming from the SO_2 is quickly canceled out by small amounts of H_2SO_4 aerosol. Large (10 μm), warming aerosols (not shown), require larger concentrations in order to arrive at an optical depth of 10 (still less than 5 ppmv).

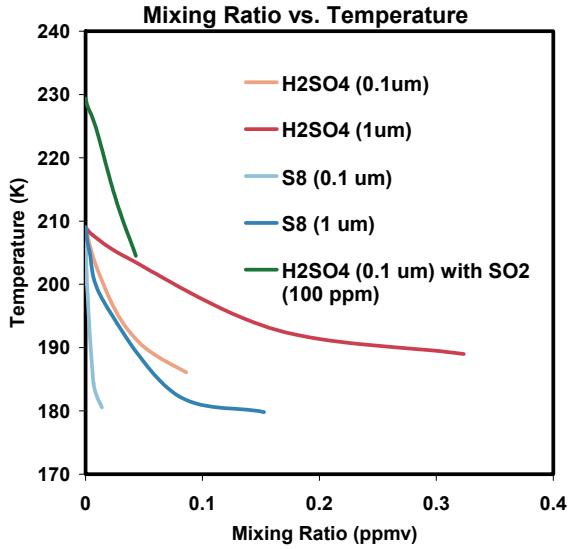

Figure 6.

Conclusions: From these results we can make several conclusions:

(1) SO_2 and H_2S gases, considered alone, would warm the surface of Mars. A hot, enduring greenhouse is unlikely, but concentrations of SO_2 up to several hundreds to thousands of ppmv would be sufficient to bring temperatures above freezing for certain regions during certain portions of the year. This is true of atmospheres up to 2 bars (the thickest atmosphere tested).

(2) Regions with the highest percentage of time above freezing do not coincide with highest concentrations of valley networks, nor do they coincide with areas with a higher abundance of aqueous minerals. Areas where valley networks are common are among those with the least number of days above freezing.

(3) Even a small amount (<0.05 ppmv) of H_2SO_4 production in common size ranges would cancel out SO_2-derived warming. S_8 would cause cooling in the small particle range, but warming if particles could grow to more than 3 μm.

References: [1] Sharp, R.P., Malin, M.C. (1975) GSA Bull. 86, 593-609. [2] Baker, V.R. et al. (1991) Nature 352, 589-594. [3] Squyres, S.W., Kasting, J.F. (1994) Science 265, 744-749. [4] Andrews-Hanna, J. et al., 2010 JGR 115, E06002. [5] Ehlmann, B. et al. (2011) Nature 479, 53-60. [6] Haberle, R.M. (1998) JGR 103, 28,467-28,479. [7] Forget, F. et al. (2013) Icarus 222, 81-99. [8] Bibring, J-P. et al., Science 312, 400-404. [9] Carr, M.H. (1996) *Water on Mars*. Oxford Univ. Press, 229pp. [10] Fassett, C.I., Head, J.W. (2008) Icarus 198, 37-56. [11] Fassett, C.I., Head, J.W. (2008) Icarus 195, 61-89. [12] Hynek, B.M., Phillips, R.J. (2001) Geology 29, 407-410. [13] Craddock, R.A., Howard, A.D. (2002) JGR 107, 5111. [14] Halevy, I. et al. (2007) Science 318, 1903-1907. [15] Segura, T.L., et al. (2002) Science 298, 1977-1988. [16] Halevy, I., and Head, J.W. (2012) LPSC 43, Abs. 1908. [17] Goldspiel, J.M., Squyres, S.W. (1991) Icarus 89, 392-401. [18] Postawko, S.E., Kuhn, W.R. (1986) LPSC Proc. 91, D431-D438. [19] Mischna, M.A., et al. (2013) J. Geophys. Res. 118, 560-576. [20] Johnson, S.S., et al. (2008) JGR 113, E08005. [21] Tian, F., et al. (2010) EPSL 295, 412-418. [22] Wordsworth, R et al. (2011) Astrophys. J. Lett. 733:L48. [23] Wordsworth, R., et al. (2013) Icarus 222, 1-19. [24] Hummel, J.R., et al. (1988) AFGL-TR-88-0166, Hanscom AFB. [25] Palmer, K. F., Williams, D. (1975) Applied Optics 14, 208-219. [26] Fuller et al. (1998) *Handbook of Optical Constants of Solids*, Vol. 3, Academic Press, pp. 899-922. [27] Manabe, S., Wetherald, R.T. (1967) J. Atmos. Sci. 24, 241-259. [28] Pollack, J., et al. (1987) Icarus 71, 203-224. [29] Boucher, O., Anderson, T.L. (1995) J. Geophys. Res. 100, 26,177-26,134. [30] Young, A.T. Icarus 32, 1-26.